Improvement of Hydraulic Assemblies Through Analysis of the Impact of Groove Geometry on O-Ring Seals

EL Mehdi EL Bahloul[1,*], Hicham Aissaoui[2] and Mohammed Diany[1]

[1]*LabSTIC, Team Advanced Science and Technology, National School of Applied Sciences of Tetouan, Abdelmalek Essaadi University, Tetouan, Morocco*
[2]*Sustainable Development Laboratory, Faculty of Science and Technology, Sultan Moulay Sliman University, Beni Mellal, Morocco*
E-mail: mehdi.elbahloul@gmail.com
[*]*Corresponding Author*

Received 28 August 2024; Accepted 09 February 2025

Abstract

This article presents a study aimed at modelling two different configurations of assemblies using an O-ring subjected to compressive loading and internal fluid pressure. The dimensions of the O-ring and the rectangular groove are determined in accordance with ISO 3601. The aim of this study is to analyse the influence of the groove shape on the mechanical behaviour of the O-ring and to evaluate the sealing performance and mechanical strength of the new groove design. The results of this analysis will provide a better understanding of the advantages and limitations of the new configuration and help optimise its use in practical applications.

Keywords: O-ring, groove, finite element model, contact pressure, fluid pressure.

International Journal of Fluid Power, Vol. 26_1, 43–64.
doi: 10.13052/ijfp1439-9776.2613

1 Introduction

Cylinder capacity is essential for assessing the performance of hydraulic systems, particularly for applications requiring increased power and precision. They are widely used in industrial, construction and automotive applications. The O-ring plays an essential role as the main seal in the hydraulic cylinder, and its sealing performance is directly linked to the correct operation of the cylinder [1]. Research into the factors that influence the sealing performance of the rubber ring is therefore crucial to accurately calculating this performance and improving the accuracy of the cylinder design. Due to the non-linear characteristics of the material, the complexity of the geometry and the contact interactions, finite element analysis (FEA) is a commonly used method to study the sealing performance of rubber O-rings [2]. Rubber materials, as hyperelastic materials, require suitable constitutive models for numerical calculations. Common models used in finite element analysis include the Arruda Boyce, van der Waals, Ogden and Mooney-Rivlin constitutive equations. A review by Ali shows that the Mooney-Rivlin model is particularly suitable for small and medium deformations [3]. This constitutive model is frequently used to accurately represent the non-linear behaviour of rubber O-rings in numerical simulations.

Huang pointed out that the seal structure is axisymmetric, which makes it possible to use a two-dimensional axisymmetric model for the numerical calculation of the sealing ring [4]. To this end, a two-dimensional axisymmetric model of the seal structure was developed using ANSYS software, and its validity was verified [5]. Finite element analysis was used to assess the behaviour of an O-ring subjected to uniform pressure levels and internal pressure.

The design of rubber seals has been extensively studied, and new types of seals have been used to provide better sealing, such as D-shaped, T-shaped, U-shaped, X-shaped, Y-shaped, reinforced O-rings, and many others. For example, the D-shaped seal has been designed to improve the contact width between the groove and the seal, and can be thought of as a half-section of an O-ring. Comparisons between the D-ring and the O-ring have shown that the D-ring offers better sealing performance in terms of maximum contact stress. However, it has the disadvantage of extrusion through the seal gap [6].

The analysis carried out by Mose on the extrusion of the D-ring under a hydraulic pressure of 5.89 MPa highlighted a risk of seal failure. The D-ring has disadvantages in terms of stress concentration in static sealing and extrusion in dynamic sealing [7]. These results highlight the sealing limitations

of the D-ring and the need to find alternatives to improve sealing performance. The geometric shape of the X-ring offers significant advantages under dynamic conditions by reducing friction. Shin's research has conclusively demonstrated that the X-seal generates a higher contact stress than the O-ring under specific conditions. However, it should be noted that the maximum allowable extrusion pressure for the X-seal is limited to 3.92 MPa [8]. A limitation of the X-seal is its reduced ability to maintain sufficient contact length under low pressure, which can compromise its sealing performance [9]. The sealing performance of the Y-seal relies on the surface area of the coupling lips, as it is a lip-type rubber seal. Cui carried out an analysis of the effect of hydraulic pressure on the sealing performance of the Y-seal. His work made it possible to determine the location of the maximum stresses and the most critical deformation zone, based on the seal failure criterion [10]. El Bahloul et al. [11, 12] have proposed improving elastomer O-rings by adding a metal core inside. This solution strengthens the structure of the seal and improves its mechanical performance and resistance to leakage. Studies have shown that reinforced O-rings show promise in reducing deformation under pressure, but it is important to choose the size of the metal core carefully to avoid excessive stress. Jahangir's findings, based on tests carried out on 21 seals, highlight a variation in the properties of these seals depending on their geometric shape and the manufacturing method used [13]. This finding highlights the importance of taking these factors into account when designing and manufacturing seals, to ensure optimum performance and increased reliability in specific applications. In an earlier study on the development of seals for pneumatic valves [14], the focus was on the design of compact, low-friction seals capable of operating without grease. Comparisons between prototypes and existing seals highlighted the evolution of environmental and industrial standards. In a study by Belforte et al. [15], the cross-sectional optimization of an elastomer seal for pneumatic cylinders was carried out to reduce the friction force. The paper uses a numerical finite element model taking into account material non-linearities and frictional contact. The proposed geometric modifications reduced friction by 50–80%, while maintaining sealing efficiency. Experimental results confirm the reliability of the numerical model, encouraging future research into pneumatic seal friction. The article by Rita Ambu et al. [16], explores the redesign of a guide bearing for pneumatic actuators, focusing on the front head/bearing interface. Using finite element analysis, the authors propose modifications that reduce wear and extend cylinder life. Tests show that these new configurations outperform commercial designs in terms of performance and durability.

Rectangular grooves were widely used for O-rings. However, some applications required solutions to prevent the O-rings from coming loose. The study by Hou et al. [17] compared the performance of O-rings in rectangular and trapezoidal grooves. Their results showed that trapezoidal grooves sometimes offered better sealing performance and stability for O-rings. This opened up new design perspectives for improving sealing systems. In an earlier study [18], the authors of this study analysed the sealing performance of static axial joints fitted with O-rings in different grooves shapes. The simulations revealed that concave grooves performed better by generating higher contact pressure on the mating surfaces, thereby reducing the risk of leakage. In addition, the maximum stresses on the seal were slightly lower in concave grooves than in rectangular grooves.

With the aim of improving the sealing performance of static radial assemblies using O-rings in hydraulic cylinders and mechanical systems, this study focuses on a detailed analysis of the sealing of elastomer O-rings. To do this, we have developed an advanced numerical model that allows us to explore the sealing characteristics of these seals in depth. In this study, we will explore the stress-strain behavior of the elastomer seal using hyperelasticity theory. In addition, we will determine the Mooney and Rivlin parameters based on reference compression tests. This approach will enable us to obtain an in-depth understanding of the mechanical behaviour of the O-ring and to analyse its sealing performance when installed in a cylindrical or rectangular concave groove. Using this methodology, we will be able to provide valuable information on the sealing performance of O-rings in different groove configurations. These results will form a solid basis for improving the design of O-rings and optimising their assembly, with the aim of achieving optimum sealing in hydraulic and mechanical applications.

2 Materials Characterization

The material used for this seal is a nitrile elastomer (NBR), widely chosen to provide an effective seal in cylinders and hydraulic systems because of its resistance to pressure. Based on the assumption of hyperelasticity theory, the strain and stress of an elastomer material are described by the strain energy density function, which is expressed as a function of the strain invariant [19].

$$W = f(I_1, I_2, I_3) \tag{1}$$

In this formulation, W represents the strain energy function, λ is the invariant of the Cauchy-Green strain tensor [20]. Furthermore, the invariants

of the Cauchy-Green strain tensor can be expressed in terms of the ratios of the principal stretches λ_1, λ_2, λ_3.

$$\begin{cases} I_1 = \lambda_1^2 + \lambda_2^2 + \lambda_3^2 \\ I_2 = (\lambda_1\lambda_2)^2 + (\lambda_2\lambda_3)^2 + (\lambda_3\lambda_1)^2 \\ I_3 = (\lambda_1\lambda_2\lambda_3)^2 \end{cases} \tag{2}$$

In addition, the Cauchy stress tensor formula σij is expressed in terms of the principal stretches.

$$\begin{cases} \sigma_1 = 2\lambda_1 \left[\dfrac{\partial W}{\partial I_1} + (\lambda_2^2 + \lambda_3^2)\dfrac{\partial W}{\partial I_2} + \lambda_2^2\lambda_3^2\dfrac{\partial W}{\partial I_3} \right] \\ \sigma_2 = 2\lambda_2 \left[\dfrac{\partial W}{\partial I_1} + (\lambda_1^2 + \lambda_3^2)\dfrac{\partial W}{\partial I_2} + \lambda_1^2\lambda_3^2\dfrac{\partial W}{\partial I_3} \right] \\ \sigma_3 = 2\lambda_3 \left[\dfrac{\partial W}{\partial I_1} + (\lambda_1^2 + \lambda_2^2)\dfrac{\partial W}{\partial I_2} + \lambda_1^2\lambda_2^2\dfrac{\partial W}{\partial I_3} \right] \end{cases} \tag{3}$$

The two-parameter Mooney-Rivlin model [21] is used to represent an approximately incompressible material. The strain energy function W is defined according to this model.

$$W = C_{10}(I_1 - 3) + C_{01}(I_2 - 3) + \left(\frac{C_{10}}{2} + C_{01}\right)\left(\frac{1}{I_3^2} - 1\right) + \frac{C_{10}(5\upsilon - 2) + C_{01}(11\upsilon - 5)}{2(1 - 2\upsilon)}(I_3 - 1)^2 \tag{4}$$

Where C_{10} and C_{01} represent the material parameters. Since the elastomer is approximately considered incompressible [22], the Poisson's ratio ν is equal to $0,499 \approx 0,5$ and I_3 is equal to 1. Therefore, the two-parameter Mooney-Rivlin model is defined as follows:

$$W = C_{10}(I_1 - 3) + C_{01}(I_2 - 3) \tag{5}$$

In addition, uniaxial compression tests,

$$\begin{cases} \lambda_1 = \dfrac{1}{\lambda_2^2} = \dfrac{1}{\lambda_3^2} = \lambda \\ \sigma_1 = 2\lambda_1 \left[\dfrac{\partial W}{\partial I_1} + (\lambda_2^2 + \lambda_3^2)\dfrac{\partial W}{\partial I_2} \right] \\ \sigma_2 = \sigma_3 = 0 \end{cases} \tag{6}$$

Where λ represents the strain value. Using Equations (5) and (6), the Cauchy stress can be developed as follows:

$$\sigma = \frac{2\lambda^4}{\lambda^3 - 1} C_{10} + \frac{2\lambda^3}{\lambda^3 - 1} C_{01} \tag{7}$$

Using the experimental elastomer compression data reported in reference [23], the Mooney-Rivlin model parameters $C_{10} = 1.84$ and $C_{01} = 0,47$ were fitted in accordance with Equation (7).

3 Modeling

3.1 Structure

O-rings are the most widely used seals in the aerosol and aerospace industries because of their efficiency, economy and ease of use. They provide a reliable seal by blocking the gap between mating surfaces, preventing unwanted fluid leakage. Their simple design and versatility in terms of size, shape and materials make them practical choices for sealing mechanical assemblies. An O-ring consists of two essential elements: the O-ring itself and the groove into which it is inserted. The groove is a precisely machined groove that accommodates the O-ring and provides a contact surface for sealing. The main components of the rod and piston grooves are shown in Figure 1. When the O-ring is correctly positioned in the groove, it is compressed when the components come into contact, creating a tight, hermetic fit. This compression eliminates any play between the components and prevents fluids

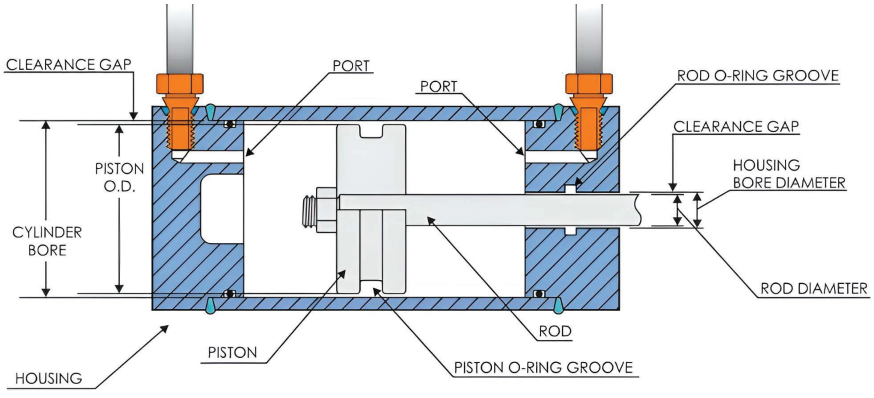

Figure 1 Seal configuration in a double-acting cylinder.

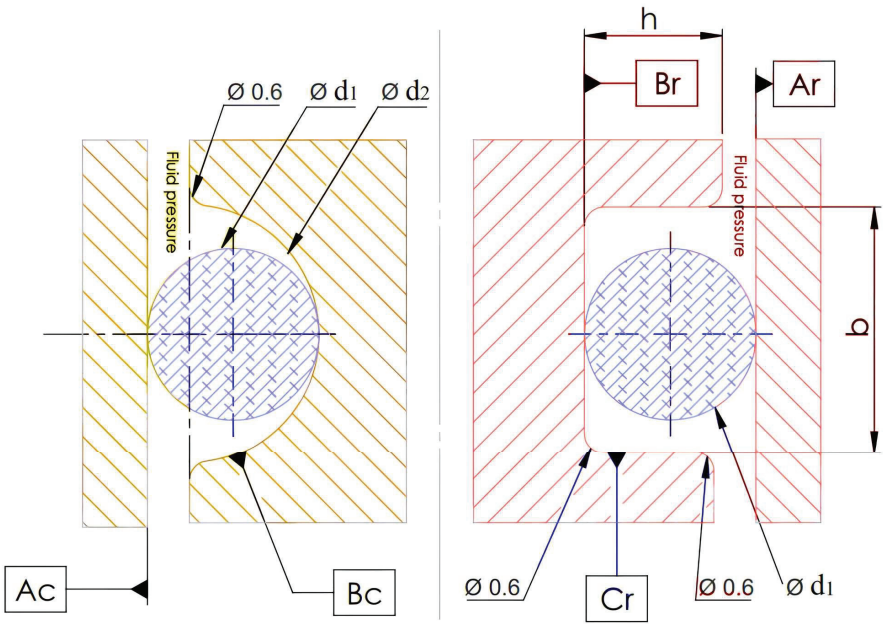

(a) (b)

Figure 2 O-ring installation in two types of groove (a) Rectangular groove (b) Concave groove.

escaping through the gap. Thanks to its flexibility and ability to deform, the O-ring adapts to surface irregularities and ensures a reliable seal. It is important to note that the quality of the groove and the O-ring, as well as the selection of the right material, are essential factors in ensuring an optimum seal.

In the work presented, the aim is to model two different configurations, as illustrated in Figure 2. involving the use of an O-ring subjected to a compressive load, representing the installation force, and to the pressure of the fluid contained within the assembly. The dimensions of the O-ring and the rectangular groove are determined on the basis of ISO 3601 [24]. The mechanical and geometric characteristics of the two assemblies are detailed in Table 1.

The present work aims to complement the previous study [18] by analysing the influence of the groove shape on the mechanical behaviour of the O-ring in radial assemblies, under real operating conditions. The analysis

Table 1 Mechanical and geometric characteristics of the assemblies

Symbol	Designation	Contact
Ac	Top surface	O-ring-plates
Ar	Bottom surface	
Bc	Top surface	O-ring-groove
Br	Bottom surface	
Cr	Lateral surface	
		Values
b	Width of the rectangular groove	3.6 mm
D	O-ring inner diameter	17,96 mm
d_1	O-ring cross-section diameter	2,65 mm
d_2	Diameter of the concave groove	4 mm
E	Young's modulus of elastomer	13,85 MPa
h	Height of the groove	4.2 mm
ν	Poisson's ratio of the O-ring	0,499
μ	Friction coefficient	0.2

focuses on assessing the impact of the new groove shape on the seal's performance in terms of sealing and mechanical strength. This study will provide a better understanding of the advantages and limitations of the new groove design, and help optimise its use in practical applications.

3.2 Finite Element Model

In order to study and compare the mechanical behaviour of an O-ring installed in a concave groove and a rectangular groove, an axisymmetric finite element model was developed using ANSYS software [25]. To ensure accurate representation of the interactions between the various components, all the elements of the assembly were meshed with rectangular elements. The O-ring was modelled by a disc using 2D planar elements with four nodes (PLANE182). The analysis carried out is static with geometric non-linearity (NLGEOM, ON) and solution control (SOLCONTROL, ON) to take account of large deformations. To simulate the contact between the elements in contact, CONTA171 and TARGE169 contact elements were used. They are based on the 2D 2-Node Surface-To-surface contact approach. In addition, a friction interaction was defined for the contact pairs using the MP command. The contact formulation used is the "Lagrange multiplier on contact-normal and penalty-on-tangent"(KEYOPT (2) = 3 on CONTA171), allowing contact forces to be modelled efficiently.

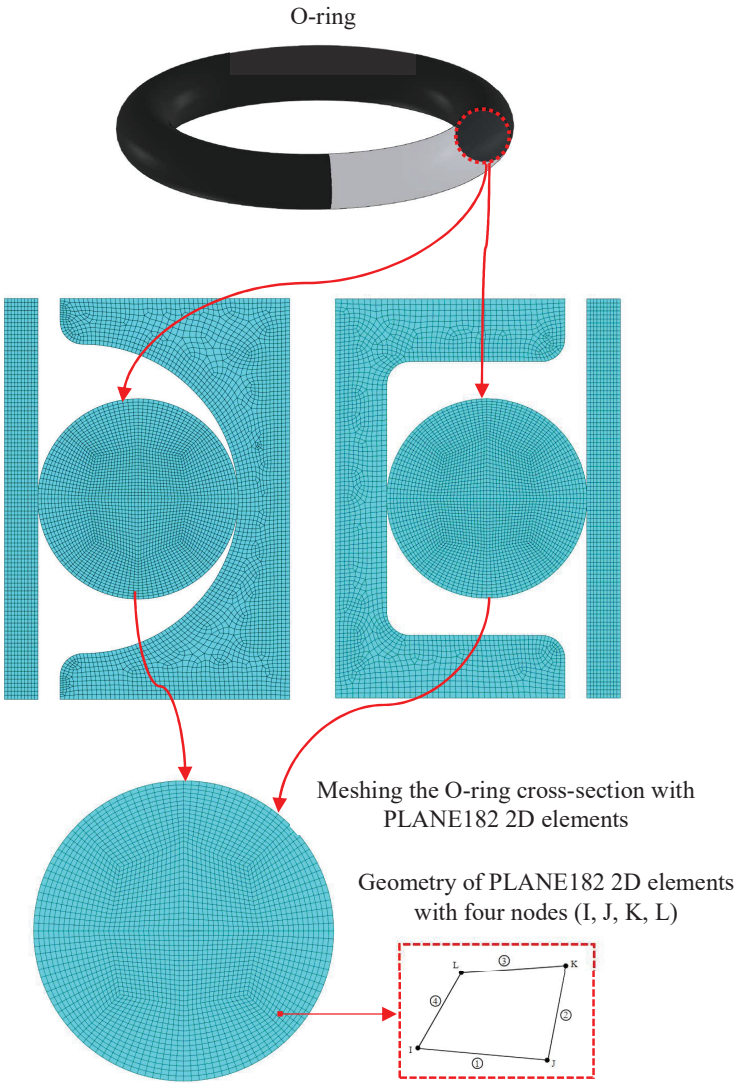

Figure 3 Finite element modeling, in a static study, of two types of installation: rectangular groove and concave groove.

Figure 3 illustrates the mesh configuration used for the seal in both installations, demonstrating the quality and accuracy of the mesh for the analysis. Using this finite element model, it will be possible to analyse in detail the mechanical behaviour of the O-ring in both groove configurations,

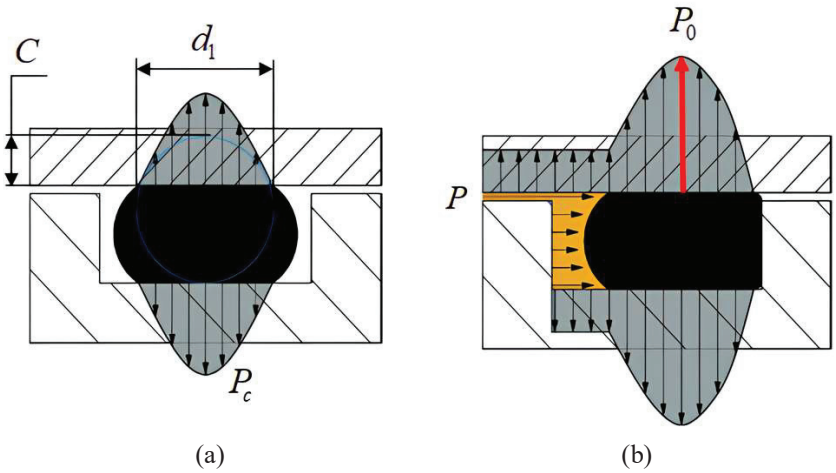

Figure 4 Sealing mechanism for static O-rings (a) Initial compression of the seal (b) Seal under pressure of the fluid to be sealed.

providing valuable information on the seal's performance in terms of sealing and mechanical strength.

3.3 Installation and Working Mode

The Challenger space shuttle disaster on 28 January 1986 was caused by the faulty design of an elastomer O-ring [26]. This accident served as a lesson in improving seal design, underlining the importance of reliability and rigorous testing procedures.

The sealing mechanism of an elastomer O-ring is based on the elasticity and incompressibility of the material. The basic sealing phenomenon is best explained by considering an O-ring with a circular cross-section (Figure 4). From an initial diameter d_1, in its free state, the O-ring is compressed during assembly by an amount defined as the compression ratio C. Consequently, after installation, the contact surfaces between the seal and the structure produce a contact pressure P_c.

During operation, the pressure of the fluid P acts on the exposed surface of the seal and causes the contact pressure to rise to a higher value. The maximum contact pressure P_0 exceeds the pressure of the fluid to be sealed P. If this were not the case, the fluid could penetrate the gaps between the seal and the contact surface, resulting in a leak.

The physical interpretation of the above is that, when the elastomer O-ring is subjected to initial compression and exposed to fluid pressure, it behaves

like a liquid with a very high surface tension. The seal thus maintains the clamping force and transfers the fluid pressure to the sealing contact [27].

4 Results and Discussion

Before proceeding with the analysis of the two installations, it is essential to carry out numerical tests in order to verify the influence of the mesh density on the simulation results. With this in mind, four different mesh sizes were proposed, referred to respectively as Mesh 1 (300 elements), Mesh 2 (1,200 elements), Mesh 3 (2,700 elements) and Mesh 4 (4,800 elements).

Figure 5 shows the Von Mises stress distribution inside the O-ring, obtained using the FE model shown in Figure 3. The numerical tests were carried out with the same mechanical and geometric characteristics, a compression ratio of 10% and a fluid pressure of 5 MPa. The simulation results show almost identical stress distributions for the four meshes tested.

It is also observed that an increase in mesh size leads to an increase in the error on the maximum value of the equivalent Von Mises stress calculated. On the other hand, a smaller mesh size leads to a significant increase in computation time. Consequently, in the continuation of our study, we will adopt "Mesh 3", composed of 2,700 elements, which offers an adequate compromise between the accuracy of the results and the calculation time.

As the compression ratio of the seal increases, it adopts a behaviour similar to that of an incompressible fluid, which leads to an increase in the contact pressure intensity at the surfaces likely to cause leaks. The contact pressure profiles of the contact surfaces Ar, Br, Ac and Bc are shown in Figure 6, for three different values of compression ratio, noted C.

This figure shows the effect of installing the seal in a concave groove rather than a rectangular groove. It is clearly observed that, for a given compression ratio, the contact pressure when the seal is installed in the concave groove is higher than in the case of a rectangular groove, for the contact surfaces Ac and Ar. However, this is reversed for contact surfaces Bc and Br.

These results underline the importance of the groove configuration in the contact pressure intensity. Installing the seal in a concave groove results in higher contact pressures at the Ac and Ar contact surfaces, while choosing a rectangular groove results in higher contact pressures at the Bc and Br contact surfaces.

This observation highlights the significant impact of groove geometry on seal performance, and suggests that the choice of groove configuration should be carefully considered in seal design and installation.

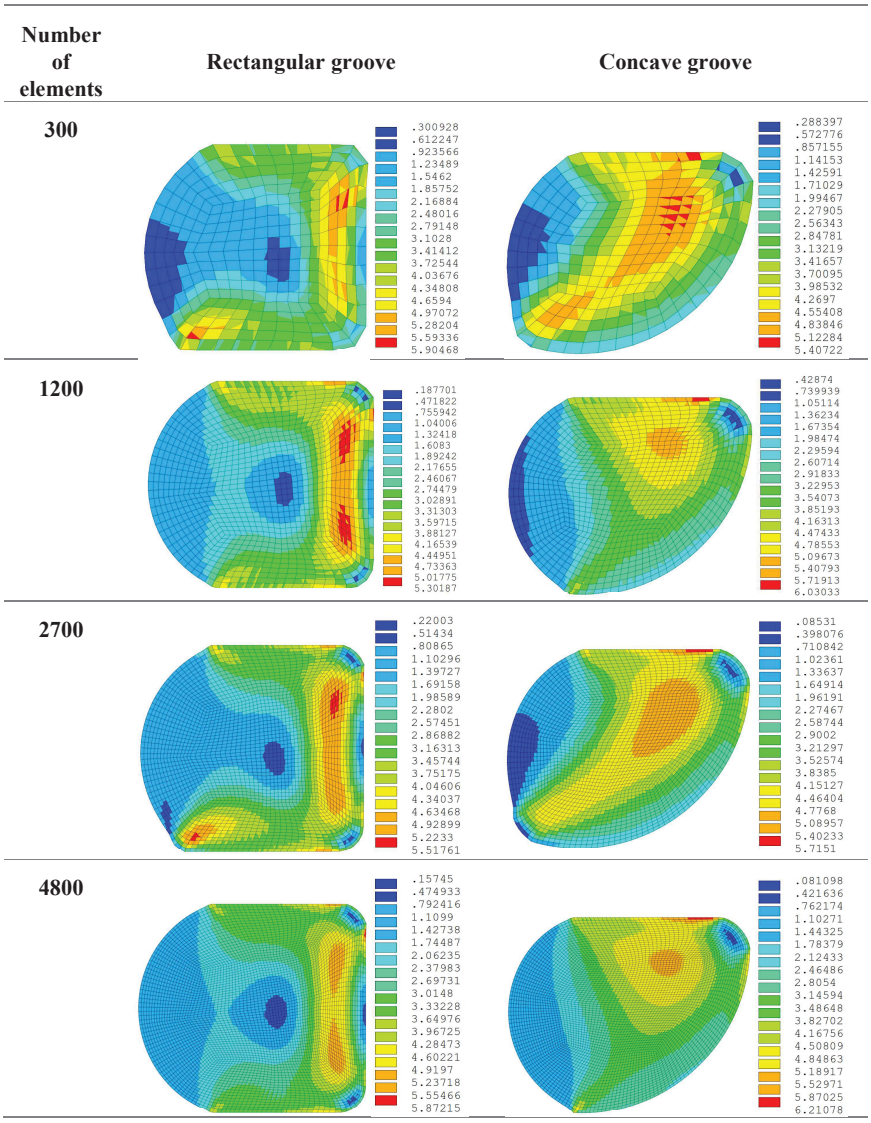

Figure 5 Von Mises stress distribution inside the O-ring for different mesh sizes.

The O-ring is widely used to prevent leakage or the passage of fluid from one compartment to another. During assembly, the seal is compressed radially to create a contact pressure distribution that ensures sealing when the assembly is subjected to pressure. The deformation and behaviour of the seal

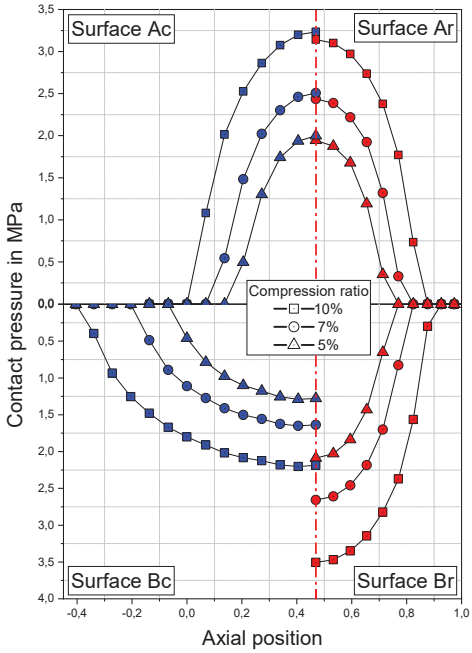

Figure 6 Comparison of contact pressure distribution without fluid pressure in rectangular and concave grooves.

under fluid pressure plays a crucial role in the sealing effectiveness of the assembly.

Figures 7, 8 and 9 illustrate in detail the contact pressure distributions for three different values of fluid pressure, taking into account the two types of groove studied. Whatever the contact surface considered, an increase in contact pressure is observed as the fluid pressure increases. It is interesting to note that the difference between the two configurations remains relatively small in terms of contact surfaces.

However, an important observation emerges from these results: the concave groove generates a larger contact surface for the Bc contact surface than for the Br surface. This significant difference between the two configurations highlights the impact of groove geometry on contact pressure distribution. The use of a concave groove therefore provides a larger contact area and, potentially, a better seal at the Bc surface compared to the rectangular groove configuration (Br).

These findings are of major importance to O-ring design, as they highlight the crucial influence of groove geometry on sealing performance. It is

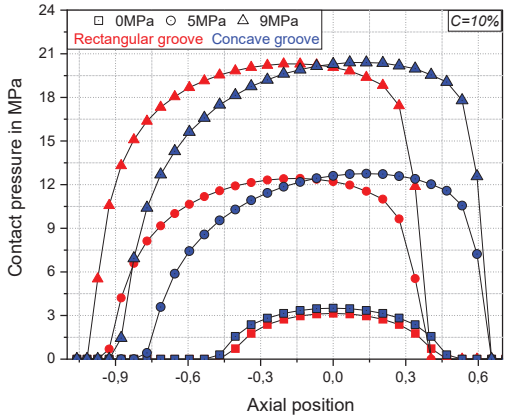

Figure 7 Comparison of contact pressure variation in Ac and Ar surfaces as a function of fluid pressure variation.

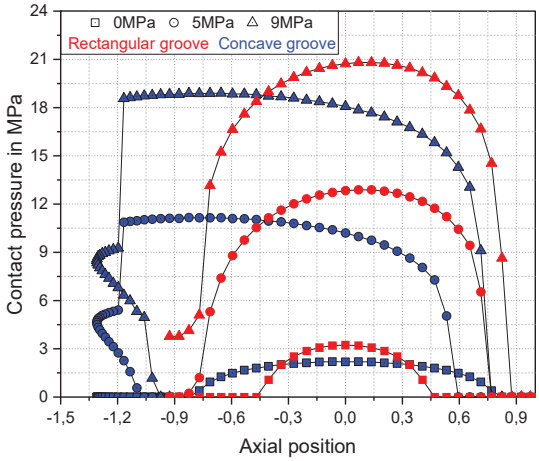

Figure 8 Comparison of contact pressure variation in Bc and Br surfaces as a function of fluid pressure variation.

essential to take these aspects into account when designing and installing O-rings to ensure effective sealing in practical applications.

Figure 10 shows the variation of the maximum contact pressure at the Ar, Br, Cr, Ac and Bc surfaces defined in Figure 2, for a compression ratio of 10%, as a function of the pressure of the confined fluid. It is clearly observed that the maximum contact pressure is always higher than the applied fluid pressure.

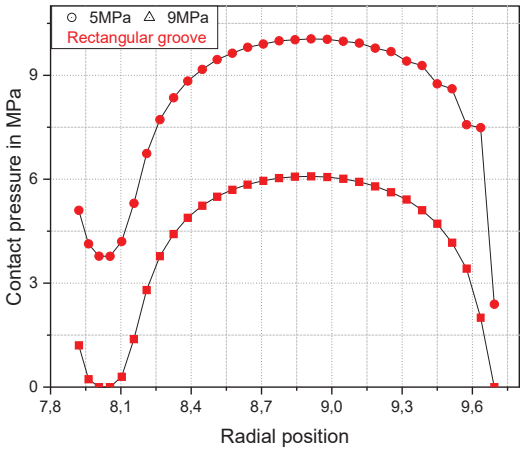

Figure 9 Variation of contact pressure in Cr surfaces as a function of fluid pressure variation.

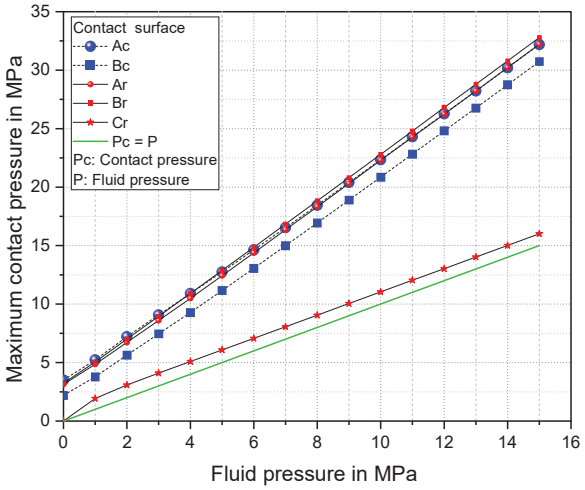

Figure 10 Influence of fluid pressure variation on maximum contact pressure in the two grooves.

However, it should be noted that the maximum contact pressures of the surfaces corresponding to the rectangular groove are slightly higher than those of the contact surfaces of the concave groove, with the exception of the Cr contact surface which produces a low contact pressure. This observation suggests the possibility of leakage if the Br contact surface fails to maintain the seal.

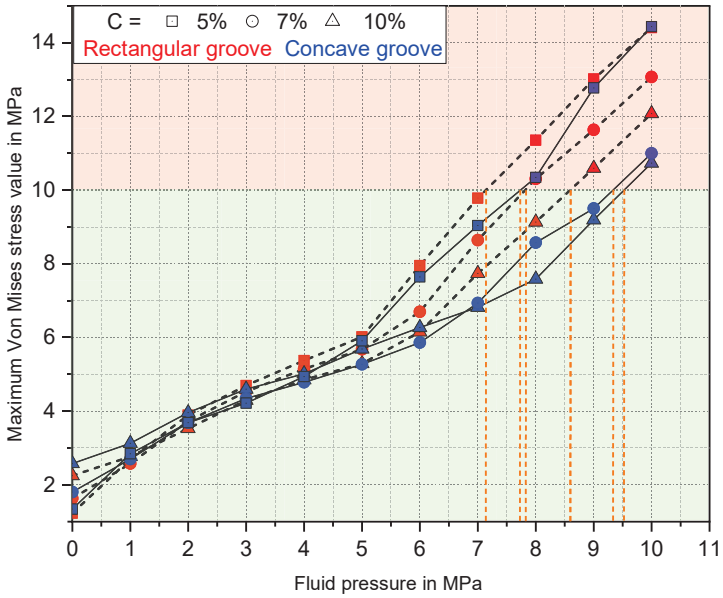

Figure 11 Effect of fluid pressure on the variation in maximum Von Mises stress.

In summary, the results indicate that the two groove configurations, rectangular and concave, offer almost identical sealing performance in terms of maximum contact pressure.

In this study, the analysis of the stress distribution inside the O-ring during the two loading phases makes it possible to locate the zones where the limit stress is reached. Figure 11 shows the variation of the maximum value of the Von Mises stress inside the seal for the two assemblies, as a function of the fluid pressure for the three compression ratios of 5, 7 and 10%.

For both assemblies, it is observed that the maximum Von Mises stress increases with increasing compression ratio as the fluid pressure increases. In addition, for a fluid pressure of less than 5 MPa, the two assemblies show remarkably little deviation for all compression ratios. However, when the fluid pressure exceeds this value, it can be seen that the higher the compression ratio, the lower the value of the maximum Von Mises stress inside the seal. In addition, it can be seen that the concave groove generates less stress for all three compression ratio values.

This behaviour can be attributed to the specific geometry of the concave groove, which allows the circular-section joint to adapt better to the shape of the groove, resulting in greater deformation and, consequently, lower stresses.

Table 2 O-ring loading limits: Table of recommended values

	Compression Ratio	Fluid Pressure
Concave groove	5%	$\leq$ 7.75MPa
	7%	$\leq$ 9.3 MPa
	10%	$\leq$ 9.5 MPa
Rectangular groove	5%	$\leq$ 7.15 MPa
	7%	$\leq$ 7.8 MPa
	10%	$\leq$ 8.6 MPa

The results clearly demonstrate the significant importance of groove geometry in stress distribution within the O-ring. A concave groove seems to significantly favour a reduction in maximum stresses, which can have beneficial effects on the durability and overall performance of the seal, particularly under conditions of high pressure. Thus, by taking into account the specific material of the seal, ISO 3601-5 [28] provides valuable guidance on the value of the maximum stress that can lead to seal failure.

In addition, curves similar to those shown in Figure 11 can be used to determine the fluid pressure that will cause the O-ring to deteriorate at a given compression ratio. In the case of the material used in Figure 11, which is NBR, the maximum permissible stress is established at 10 MPa. This value means that the seal can be used under the loading conditions specified in Table 2.

5 Conclusion

This study provided an in-depth analysis of the impact of groove geometry on O-ring performance in static radial assemblies, comparing two configurations: a rectangular groove and a concave groove. The results show that the concave groove offers significant advantages in terms of sealing performance, generating higher contact pressures on the Ac and Ar surfaces, which enhances sealing and reduces the risk of leakage. In addition, this configuration reduces maximum internal stresses, notably the Von Mises stress, which could prolong seal life under high pressure conditions.

However, the concave groove also presents certain limitations. It generates lower contact pressures on surfaces Bc and Br, which could compromise sealing in these areas. These observations underline the importance of selecting the groove shape according to the specific requirements of the application, particularly in terms of expected sealing and mechanical stresses experienced by the seal.

In short, although the concave groove improves stress distribution and sealing in certain areas, it is not a universal solution. Its use must be carefully optimized according to the service conditions and requirements of each application. These results provide a promising basis for improving O-ring design in hydraulic and mechanical systems, and pave the way for future experimental studies to validate and extend these observations.

Disclosure Statement

No potential conflict of interest was reported by the authors.

References

[1] D. Zeng et al., "Corrosion mechanism of hydrogenated nitrile butadiene rubber O-ring under simulated wellbore conditions," *Corrosion Science*, vol. 107, pp. 145–154, 2016.

[2] E. Criterion, A. Kömmling, M. Jaunich, P. Pourmand, and D. Wol, "Analysis of O-Ring Seal Failure under Static Conditions and Determination of," 2019.

[3] Ali, "A Review of Constitutive Models for Rubber-Like Materials," *American Journal of Engineering and Applied Sciences*, vol. 3, no. 1, pp. 232–239, 2010.

[4] Z. Huang and G. Li, "Optimization of cone bit bearing seal based on failure analysis," *Advances in Mechanical Engineering*, vol. 10, no. 3, pp. 1–12, 2018.

[5] E. El Bahloul, H. Aissaoui, M. Diany, E. Boudaia, and S. Touairi, "Finite Element Analysis of the O-ring Behavior Under Uniform Squeeze Levels and Internal Pressure," *WSEAS Transactions on Applied and Theoretical Mechanics*, vol. 17, pp. 226–234, 2022.

[6] C. Zhou, G. Chen, and P. Liu, "Finite Element Analysis of Sealing Performance of Rubber D-Ring Seal in High-Pressure Hydrogen Storage Vessel," *Journal of Failure Analysis and Prevention*, vol. 18, no. 4, pp. 846–855, 2018.

[7] B. R. Mose, J. S. Hawong, and J. H. Nam, "Stress analysis of a stepped rounded D-ring with a ratio of H 1/H2 = 3.0 under uniform squeeze rate and internal pressure by photoelastic experimental hybrid method," *Materialwissenschaft und Werkstofftechnik*, vol. 44, no. 10, pp. 861–878, 2013.

[8] D. C. Shin, J. S. Hawong, S. W. Lee, A. O. Bernard, and H. S. Lim, "Contact behavior analysis of X-ring under internal pressure and uniform squeeze rate using photoelastic experimental hybrid method," *Journal of Mechanical Science and Technology*, vol. 28, no. 10, pp. 4063–4073, 2014.

[9] A. O. Bernard, J. Hawong, D. Shin, and B. Dong, "Contact behavior analysis of elastomeric x-ring under uniform squeeze rate and internal pressure before and after forcing-out using the photoelastic experimental," vol. 29, no. 5, pp. 2157–2168, 2015.

[10] K. Cui, J. Qin, C. Di, and Y. Yang, "Finite Element Analysis and Simulation of the Sealing Performance of Y-ring Rubber Seal," pp. 1379–1383, 2014.

[11] E. M. EL Bahloul, M. Diany, H. Aissaoui, E. Boudaia, and M. Mabrouki, "Finite Element Analysis of O-ring Performance Reinforced by a Metallic Core," *International Journal of Fluid Power*, vol. 23, pp. 237–252, 2022.

[12] E. M. El Bahloul, H. Aissaoui, M. Diany, E. Boudaia, and M. Mabrouki, "Performance Analysis of a Pressurized Assembly with a Reinforced O-ring," *International Journal of Fluid Power*, vol. Vol. 24 4, Nov. 2023.

[13] J. Of and C. Engineering, "Joint seals for hydraulic structures in severe climates," vol. 20, no. 1, pp. 38–46, 2014.

[14] G. Belforte, M. Conte, A. Manuello, and L. Mazza, "Performance and behavior of seals for pneumatic spool valves," *Tribology Transactions*, vol. 54, no. 2, pp. 237–246, 2011.

[15] G. Belforte, A. Manuello, and L. Mazza, "Optimization of the cross section of an elastomeric seal for pneumatic cylinders," *Journal of Tribology*, vol. 128, no. 2, pp. 406–413, 2006.

[16] R. Ambu, A. M. Bertetto, and L. Mazza, "Re-design of a guide bearing for pneumatic actuators and life tests comparison," *Tribology International*, vol. 96, pp. 317–325, 2016.

[17] M. Hou, M. Su, Y. Liu, and Z. Gui, "Analysis of a dovetail O-ring groove performance," *Sealing Technology*, vol. 2010, no. 8, pp. 9–12, 2010.

[18] E. El Bahloul, M. Diany, H. Aissaoui, E. Boudaia, and M. Mabrouki, "Analysis of the Sealing Performance of a Concave O-Ring Groove," *International Review of Mechanical Engineering*, vol. 15, no. October, pp. 530–537, 2021.

[19] G. Orzechowski and J. Fra, "Nearly incompressible nonlinear material models in the large deformation analysis of beams using ANCF," pp. 451–464, 2015.

[20] H. Xu, "Nonlinear Material Design Using Principal Stretches," vol. 34, no. 4, 2015.
[21] L. Mullins, *Engineering With Rubber.*, vol. 17, no. 12. 1987.
[22] H. Yang, X. Yao, Y. Ke, Y. Ma, and Y. Liu, "Constitutive behaviors and mechanical characterizations of fabric reinforced rubber composites," vol. 152, pp. 117–123, 2016.
[23] Y. Zhou et al., "Cone bit bearing seal failure analysis based on the finite element analysis," *Engineering Failure Analysis*, vol. 45, pp. 292–299, 2014.
[24] "ISO 3601, Fluid power systems – O-rings. Part 1: Inside diameters, cross-sections, tolerances and designation codes. Part 2: Housing dimensions for general applications. Part 3: Quality acceptance criteria. Part 4: Anti-extrusion rings (back-up rings). Pa."
[25] V. 19. 2. ANSYS, ANSYS Standard Manual.
[26] "NASA - STS-51L Mission Profile | NASA." [Online]. Available: https://www.nasa.gov/mission_pages/shuttle/shuttlemissions/archives/sts-51L.html. [Accessed: 01-Aug-2023].
[27] H. K. Müller and B. S. Nau, *Fluid sealing technology: principles and applications*. Routledge, 2019.
[28] I. March, "BSI Standards Publication Fluid power systems — O-rings Part 5 : Specification of elastomeric materials for industrial applications," no. March, 2015.

Biographies

EL Mehdi EL Bahloul holds a Ph.D. in Mechanical Engineering from Sultan Moulay Slimane University, Faculty of Sciences and Technology, in Beni Mellal, Morocco. He is currently an Assistant Professor at Abdelmalek Essaâdi University in Tetouan, Morocco. Previously, he earned his Master's

degree in Mechanical Engineering from the Higher Normal School of Technical Education, Mohammed V University, in Rabat, Morocco. His primary research interests include mechanical engineering, structural mechanics, and materials science.

Hicham Aissaoui is a Professor in the Faculty of Sciences and Technologies in Electrical Engineering department at the University of Sultan Moulay Slimane, where he has been a faculty member since 1996. He completed his Ph.D. at University Mohamed V and got his Habilitation at the University of Sultan Moulay Slimane. His research interests stability analysis and nonlinear control. He had collaborated actively with researchers in several other disciplines of signal and image analysis, particularly medical images on problems at tumor diagnostics.

Mohammed Diany Ph.D. is a Professor at Mechanical Engineering Department, University Sultan Moulay Slimane, Faculty of Sciences and Technics, Beni Mellal, Morocco. His Ph.D. thesis in 2010 was on the subject of Characterization and Modelling of Stuffing Box Packings and completed at École de Technologie Supérieure, Montreal, Canada. His researches are focused on Mechanical Engineering, Structural Mechanics, and Material Sciences.